Leakage Current Mitigation in Transformerless Z-Source/Quasi-Z-Source PV Inverters

An Overview

Yuan, Jing; Yang, Yongheng; Blaabjerg, Frede

Published in:
Proceedings of 2019 IEEE Energy Conversion Congress and Exposition (ECCE)

DOI (link to publication from Publisher):
10.1109/ECCE.2019.8911827

Publication date:
2019

Document Version
Early version, also known as pre-print

Leakage Current Mitigation in Transformerless Z-Source/Quasi-Z-Source PV Inverters: An Overview

Jing Yuan, Yongheng Yang, and Frede Blaabjerg
Department of Energy Technology, Aalborg University, Denmark
Email: yua@et.aau.dk, yoy@et.aau.dk, fbl@et.aau.dk

***Abstract*—The Z-Source Inverter (ZSI) and quasi-Z-Source Inverter (qZSI) are single-stage configurations with high boosting ratios. They might be promising solutions for transformerless PV systems, requiring a high-step voltage conversion. The lack of galvanic isolation becomes the new challenge. High common mode voltages (CMV) may appear and thus potentially induce electrical hazards. To address this issue, topological and modulation strategies have been extensively discussed in the literature. However, it still lacks a general benchmark. In this paper, prior-art solutions for leakage currents mitigation in ZSI/qZSI-fed PV systems are reviewed. It serves to initiate further research to advance the performance of transformerless ZSI/qZSI-fed PV systems.**

***Index Terms*—Z-source inverter, common mode voltage, leakage currents, transformerless PV systems**

I. Introduction

Solar energy as a promising renewable energy source is widely used in grid-connected systems [1]. Traditional PV systems employ transformers to achieve galvanic isolation and also voltage boosting in certain cases [2]–[5]. However, the multi-stage configuration decreases the overall system efficiency and increases the weight and size. Transformerless PV inverters were thus developed in the literature to tackle the issues [5]–[13]. However, leakage currents appear due to the lack of galvanic isolation [10]. To address this, various mitigation strategies were proposed by modifying the topologies or modulation methods to maintain a constant common mode voltage (CMV) and decrease the common mode current (CMC) [14]–[17].

In recent years, many efforts have been made to overcome the CMV/CMC problems in transformerless PV systems. One class of mitigation methods are based on modified traditional topologies by adding more switches or passive components. In [18], the two additional switches are placed in series on the DC rails of the traditional three-phase inverter to reduce the CMV. H7 topology with seven switches was also applied in three-phase grid-connected systems for the CMV mitigation [6], [7]. In [11], a topology derived from the single-phase zero-voltage state rectifier was proposed, which can achieve a constant CMV to eliminate the leakage current. Moreover, the inverter topologies, such as H5 [12], [19], H6 [20], [21] and H8 [13], [22] can reduce the leakage current by clamping the common mode voltage to the mid-point.

In addition to the topology-based strategies, another possible solution is modulation-based [23]–[27]. In [24], the active zero state pulse-width modulation (PW) was proposed based on two active vectors replacing the traditional zero states in opposite directions, where the peak value of the CMV is reduced. Moreover, the near state PWM (RSPWM) in [25] was another modulation method which use three nearby voltage vectors to generate the reference vector. In [27], the remote state PWM was proposed where only the even vectors or odd vectors are used. Thus, the CMV remains constant.

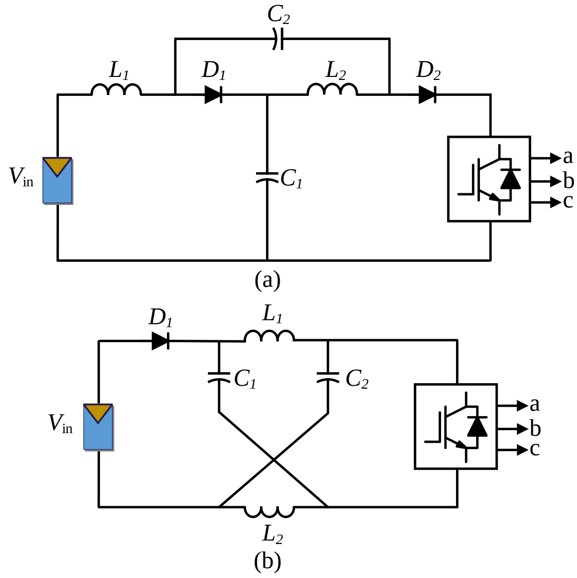

Fig. 1. Traditional impedance-source topologies: (a) Z-source inverter [28] and (b) quasi Z-source inverter [29].

Traditional transformerless grid-connected PV systems are usually two-stage solutions, including a DC-DC step-up converter and a DC-AC inverter, which have higher complexity and losses. To tackle this problem, the impedance source inverter can be adopted as an effective single-stage solution with extraordinary performance in terms of high step-up conversion ratio and low voltage stresses. The original impedance source converter is known as the Z-source inverter (ZSI) [28], which is shown in Fig. 1(a). The quasi Z-source inverter (qZSI) is shown in Fig. 1(b) [29], which achieves continuous input currents compared with ZSI. In recent years, ZSI/qZSI are gradually employed in transformerless PV systems. Similar to the transformerless PV systems based on traditional voltage source inverters (VSI), transformerless ZSI/qZSI grid-connected inverters still have the problem of leakage currents caused by CMV fluctuations. However, the prior-art solutions for the traditional VSIs are not suitable in the transformerless ZSI/qZSI PV systems. The reason is that there is a shoot-through state in the ZSI/qZSI, where the two switches in one leg are turned on simultaneously (i.e., short circuited). Compared with traditional transformerless PV systems without a high boosting capability, the inductors in the ZSI/qZSI can store the energies during the shoot-through states, so that the DC-link voltage can be boosted in the non-shoot-through states. In all, the modulation strategies proposed in the literature cannot be applied to the ZSI/qZSI systems due to the different operation principles.

Although topological and modulation strategies have been discussed in the literature to improve the performance, it still lacks a general benchmark. In this paper, prior-art solutions for leakage currents mitigation in the ZSI/qZSI-fed PV systems are reviewed based on topological and modulation modifications. In Section II, the operation principle and CMV characteristics of the qZSI PV system is presented. A detailed overview will be discussed in Section III. The comparsion of the selected topologies and solutions are presented in Section IV. Finally, the paper is concluded in Section V.

II. Operation Principle and Common Mode Voltage Analysis

In order to explain why the prior-art solutions cannot be applied in the impedance-source inverters, the operation principles of the transformerless ZSI/qZSI are presented in this section. In this paper, the operation principle of qZSI will be explained as an example. In addition, a CMV analysis in the qZSI is also demonstrated.

A. Operation Principle

There are two operation modes in the qZSI, i.e., the inversion mode and shoot-through mode. The equivalent circuits of the qZSI in the inversion mode and shoot-through mode are shown in Fig. 2. The inverter mode is similar to that of the conventional inverters, which has six active states and two zero states. As shown in Fig. 2(a), the capacitors of the network are charged and the energies stored in the inductors are delivered to the right side. During the shoot-through mode as shown in Fig. 2(b), the inverter is in short-circuit condition, where the switches in each leg are turned on simultaneously. The diode in the network is reverse-biased and the inductors are charged by the source. The voltage across the each leg in this state is zero due to the short-circuit mode. By applying the volt-second balance principle and Kirchhoff's votlage law based on the topologies shown in Fig. 2, the boosted DC-link voltage $V_{\rm dc}$ can be expressed as

$$V_{\rm dc} = \frac{1}{1-2D} \cdot V_{\rm in} \tag{1}$$

where D represents the duty cycle and $V_{\rm in}$ is the input voltage.

B. Common Mode Voltage Analysis

The space vector modulation (SVM) algorithm includes six active states and two zero states for a conventional VSI, as shown in Fig. 3. However, in a qZSI, seven shoot-through states are presented according to its operation principle. The CMV in a three-phase inverter can be defined as [30]

$$V_{CMV} = \frac{V_{aN} + V_{bN} + V_{cN}}{3} \tag{2}$$

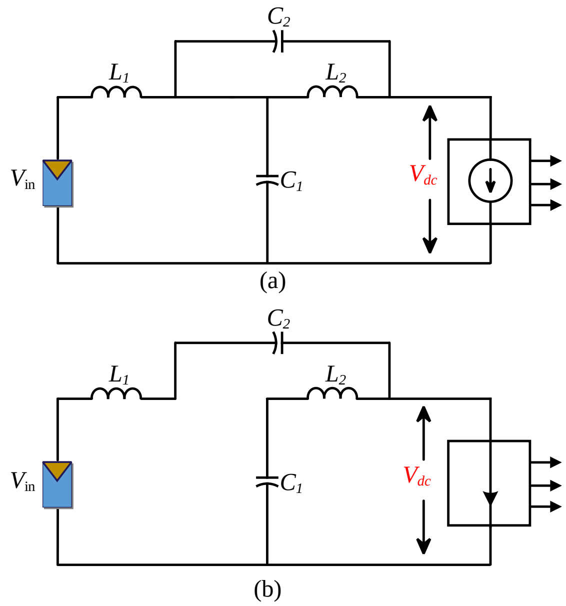

Fig. 2. Equivalent circuits of the qZSI-fed system in different modes: (a) inversion mode of and (b) shoot-through mode.

TABLE I
CMV Values in the qZSI.

Vector	CMV
V_1, V_3, V_5	$\frac{1}{3}V_{\rm dc}$
V_2, V_4, V_6	$\frac{2}{3}V_{\rm dc}$
V_7	$V_{\rm dc}$
V_0	0
Shoot-through	0

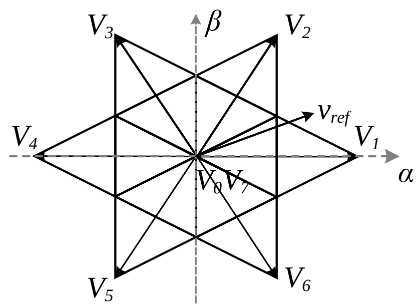

Fig. 3. Vector diagram of the conventional three-phase inverter.

with V_{CMV} being the CMV, V_{aN}, V_{bN} and V_{cN} are the inverter voltages. The lekage current can be calculated based on the obtained CMV in (2). The CMV values of different states in qZSI are presented in Table I and the states are classfied as odd vectors (V_1, V_3, V_5), even vectors (V_2, V_4, V_6), zero vectors (V_0, V_7) and shoot-through vectors. It is observed as shown in Table I that the CMV value is not identical. Therefore, the changing CMV leads to the leakage current flowing in the system. The equivelent circuit of the CMV is shown in Fig. 4 [30], [31], where C_s, L_f, and Z_{et} represents the stray capacitance, one-third of the line inductor, and ground impedance, respectively. The stray capacitance is

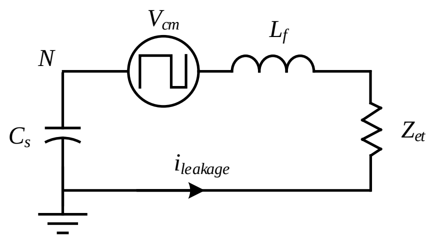

Fig. 4. Equivalent circuit for leakage current flow.

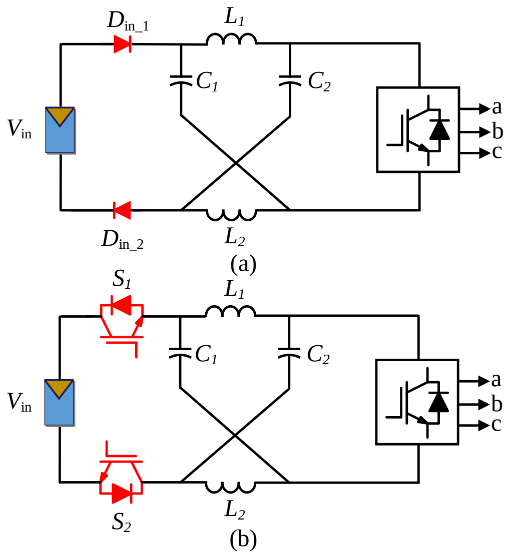

Fig. 5. Modified topologies for CMV/CMC reduction in PV systems: (a) ZSI-D [32] and (b) ZSI-S [33].

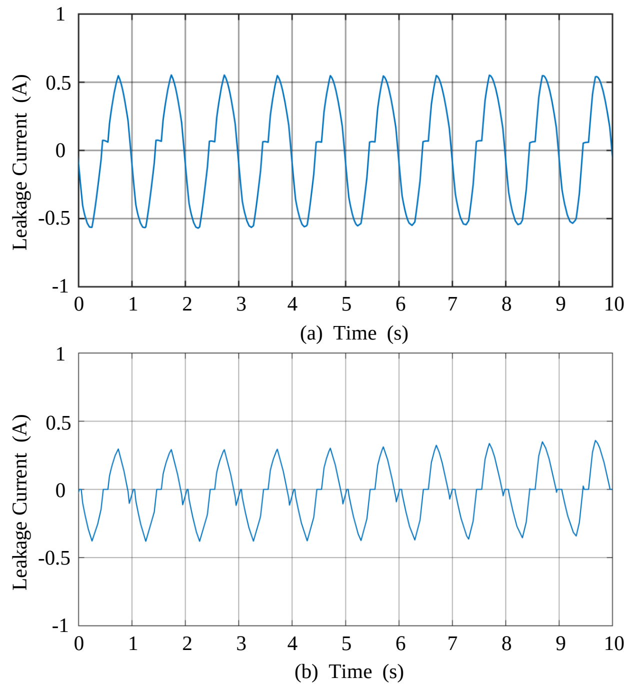

Fig. 6. Simulation results of leakage currents in the topology of: (a) ZSI and (b)ZSI-D.

usually 50-150 nF/kW [30] and the ground impedance is normally resistive with a few Ohms.

III. Overview of Mitigation Techniques for Transformerless ZSI/qZSI

A. Modified-Topologies

To mitigate the leakage current in a transformerless ZSI/qZSI PV system, adding more switches or passive components is effective. Based on the conventional ZSI topology shown in Fig. 1 (a), a modified topology by adding an additional fast-recovery diode in the ZSI (ZSI-D) is shown in Fig. 5(a) [32]. The feature of this topology is that during the shoot-through states, the additional diode provides an circulation path for leakage currents. To show the performance of the ZSI-D compared with the conventional ZSI, the simulation results of leakage currents is shown in Fig. 6. It is observed that the leakage current in Fig. 6(b) is smaller by adding the extra diode. Although the ZSI-D has better performance than the ZSI, abnormal operations may happen if the currents in diodes become negative during the non-shoot-through states. To tackle this, [33] proposed to replace the two diodes with two insulated gate bipolar transistors, as shown in Fig. 5(b). Moreover, the modified topology can ensure the system stable for wide range of the modulation index. In [9], the authors proposed a modified ZSI topology based on the Highly Efficient and Reliable Inverter Concept (HERIC), as shown in Fig. 7(a), to maintain a constant CMV in PV applications. Although two controlled switches are added into the system, the extra losses caused by these two switches are negligible considering that they operate under the line frequency. In [34], a modified HERIC qZSI topology with two extra controlled switches and diodes was proposed, as shown in Fig. 7(b). Compared with the previous HERIC-based topology, the extra two power diodes have much better switching characteristics than the anti-parallel diodes of the main power switches. The proposed topology not only eliminates the leakage currents but also achieve AC decoupling between the PV module and AC grid in the freewheeling and shoot-through states. In [30], the input inductor of qZSI is divided into two inductors, which can achieve a constant dc voltage without high harmonics using its corresponding modulation technique. Moreover, a modified topology named semi-ZSI is another alternative to be applied in PV systems to mitigate leakage currents [35], [36], as shown in Fig. 8. The advantages of the semi-ZSI over conventional ZSI/qZSI is that only two active switches are used to obtain a sinusoidal voltage. What's more, the CMV can be minimized with its ground sharing features and the overall size of the inverter can be improved by means of the coupled inductors.

B. Modulation-Based Techniques

As discussed previously, the existing modulation-based mitigation methods are not appropriate for Z-source family inverters due to the shoot-through states. Based on the above modified ZSI topologies, the corresponding modulation methods were also proposed to reduce the leakage currents in the literature.

As shown in Fig. 5(a) [32], the ZSI-D applies three specific modulation thechniques, e.g., odd PWM (OPWM), even PWM (EPWM) and odd-even PWM (OEPWM), to

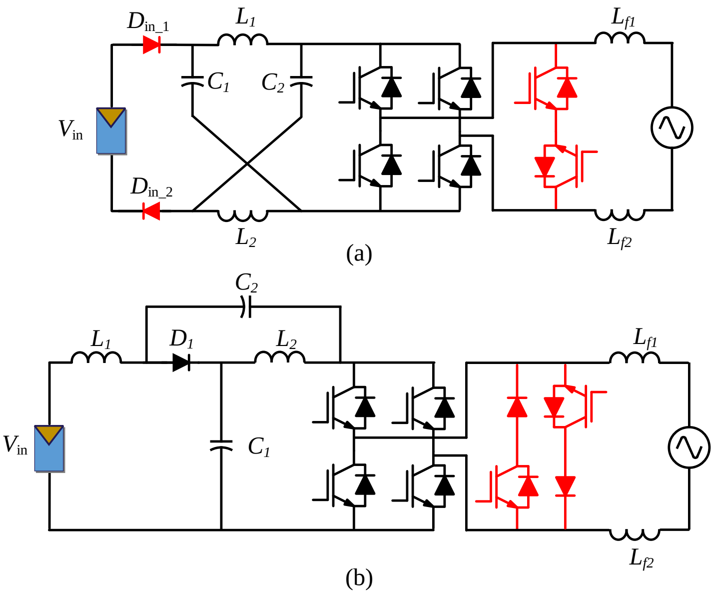

Fig. 7. Modified HERIC-based topologies for the CMV/CMC reduction in PV systems: (a) HERIC-ZSI [9] and (b) HERIC-qZSI [34] .

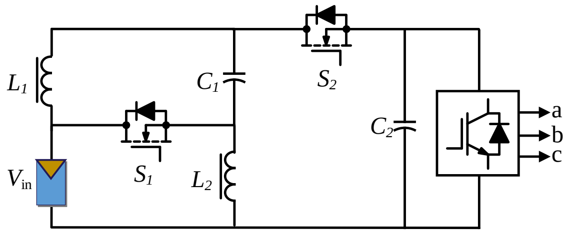

Fig. 8. Single-phase semi-ZSI [35].

guarantee a constant CMV. The principle of OPWM is that the reference voltages can be composed by utilizing odd active and single one-leg shoot-through space vectors. In addition, the PV voltage can be boosted by using these vectors. It is observed as shown in Fig. 9(a) that there are three sectors which are divided by odd active vectors and the reference voltage is composed by these three odd vectors. It is noted that the zero vectors are not considered in this modulation algorithm. Moreover, the EPWM, as shown in Fig. 9(b), is another modulation method, which utilizes the even active and one-leg shoot-through space vectors to compose the output reference voltages. Based on Table I, it is observed that the CMV is the same so that the leakage currents can be eliminated. In addition, the OEPWM, as seen in Fig. 9(c), is a combination of OPWM and EPWM, which is dependent of the position of the output reference voltage, and however, the disadvantage of OEPWM is that there are spikes in the leakage currents during each fundamental cycle due to the minor changes in the CMV.

Although the above methods can eliminate the leakage currents effectively, there are high frequency harmonics in the CMV during the shoot-through states. To tackle this, in [30], a modified OPWM technique was proposed with minor changes in qZSI topology. Moreover, a novel modulation method named constant area SVM (CASVM) is proposed in [31]. Compared with the existing mitigation methods, the advantage of the CASVM is that the effectiveness

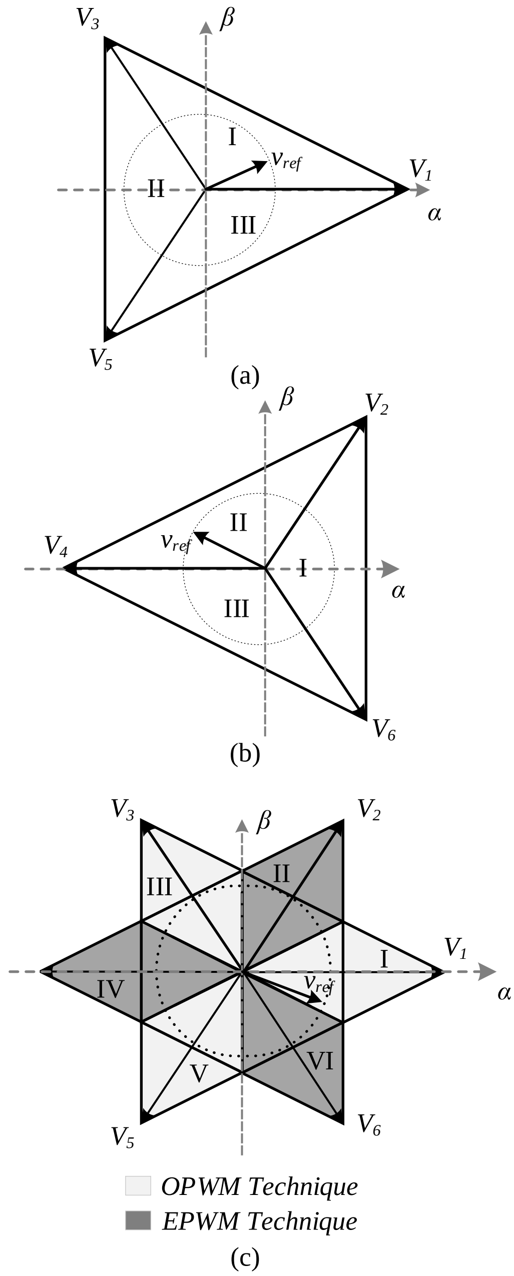

Fig. 9. Output voltage space vectors for the ZSI-D: (a) OPWM, (b) EPWM, and (c) OEPWM.

of the CASVM is not affected by CMV fluctuations and shoot-through implementation methods. Moreover, the high-frequency harmonics of the leakage currents are eliminated by adding a notch filter to the qZSI.

In additional to these modulation methods applied in traditional ZSI/qZSI topologies, certain modulation strategies were proposed for special topologies. In [8], the proposed modulation strategy, where the zero vectors are replaced by two active opposite voltage vectors, can reduce the leakage current for the Z-source four-leg transformerless PV inverter based on the ZSI-D topology. For the qZSI three-level T-type inverter ($3LT^2I$), [37] presented an effective SVM strategy to reduce the magnitude and slew rate of the CMV. The shoot-through phase can be selceted properly based on the sector number and the shoot-through states are inserted to zero vector without affecting the active states and output voltage.

IV. Comparison and analysis of selected topologies

In order to benchmark the selected topologies, a detailed comparison in terms of component counts, modulation methods, leakage currents, CMV, filter counts and efficiency, is carried out. The comparison of the selected topologies are summarized in Table II.

As it can be seen from Table II, the qZSI T-type inverter has the highest component-count compared with other topologies due to its complicated structure, which consists of two qZSI networks and more active switches. However, the semi-ZSI has the lowest component counts without using any diodes in the topology, where the coupled-inductor contributes to reducing the current ripple and cost of the system. For the choice of modulation method, the OPWM method is the most widely applied in selected topologies. When it comes to filter counts, the qZSI in [31] employs the most inductors by using the notch filter to the system and the ZSI with four legs in [8] uses up to 4 capacitors due to the more legs compard with other topologies. Finally, all the reported efficiency in the selected topogies are above 90% and the highest is 96% in [32].

The performance of those selected solutions is demonstrated in terms of the leakage currents and the CMV. It is observed in the selected topologies that the lowest leakage current is only 2 mA in the ZSI-S, and however, the largest value is up to 28 mA in the four-leg ZSI. There are only two CMV values (0 and 150 V) in the ZSI-D, and however, the ZSI-S can achieve a constant CMV and lower leakage current due to the active switches. In other selected topolgies, the CMV can be maintained a constant value based on the modified topologies or modulation methods. In this way, a low leakage current is also obtained.

Although these selected topologies by using different modulation methods have good performance, there is room for further improvements of leakage current mitigation in transformerless ZSI/qZSI systems. Firstly, the existing solutions based on modified topologies adopt a relatively large number of extra components, which lead to higher cost and potentially low reliability, and thus the new modified topologies using fewer components is a promising solution to reduce the cost and improve the reliability of the system. In addition, it is necessary to propose new modulation techniques, which are easy to be implemented in the digital control system compared with the existing complicated modulation methods.

V. Conclusion

The CMV/CMC suppression strategies of the traditional voltage source inverter are not suitable for the direct use in the ZSI/qZSI transformerless PV systems due to the shoot-through state. In this paper, the operation principle of the ZSI/qZSI and the CMV/CMC characteristics in the ZSI/qZSI-fed transformerless PV systems were presented. In addition, an extensive overview of the CMV/CMC mitigation techniques applied in ZSI/qZSI transformerless PV systems was performed. The benchmark is conducted by reviewing the modified topologies and modulation technique in the selected topologies. This review paper aims to provide a comprehensive information for the CMV/CMC mitigation techniques applied in ZSI/qZSI transformerless PV systems.

References

[1] L. Zhang, K. Sun, Y. W. Li, X. Lu, and J. Zhao, "A distributed power control of series-connected module-integrated inverters for PV grid-tied applications," *IEEE Trans. Power Electron.*, vol. 33, no. 9, pp. 7698–7707, Sep. 2018.

[2] Q. Liu, Y. Li, L. Luo, Y. Peng, and Y. Cao, "Power quality management of pv power plant with transformer integrated filtering method," *IEEE Trans. Power Del.*, vol. 34, no. 3, pp. 941–949, Jun. 2019.

[3] T. Ku, C. Lin, C. Chen, and C. Hsu, "Coordination of transformer on-load tap changer and PV smart inverters for voltage control of distribution feeders," *IEEE Trans. Ind. Appl.*, vol. 55, no. 1, pp. 256–264, Jan. 2019.

[4] T. Liu, X. Yang, W. Chen, Y. Li, Y. Xuan, L. Huang, and X. Hao, "Design and implementation of high efficiency control scheme of dual active bridge based 10 kv/1 mw solid state transformer for PV application," *IEEE Trans. Power Electron.*, vol. 34, no. 5, pp. 4223–4238, May 2019.

[5] J. Shen, H. Jou, and J. Wu, "Novel transformerless grid-connected power converter with negative grounding for photovoltaic generation system," *IEEE Trans. Power Electron.*, vol. 27, no. 4, pp. 1818–1829, Apr. 2012.

[6] T. K. S. Freddy, N. A. Rahim, W. Hew, and H. S. Che, "Modulation techniques to reduce leakage current in three-phase transformerless H7 photovoltaic inverter," *IEEE Trans. Ind. Electron.*, vol. 62, no. 1, pp. 322–331, Jan. 2015.

[7] X. Guo, "Three-phase CH7 inverter with a new space vector modulation to reduce leakage current for transformerless photovoltaic systems," *IEEE J. Emerg. Sel. Top. Power Electron.*, vol. 5, no. 2, pp. 708–712, Jun. 2017.

[8] X. Guo, Y. Yang, R. He, B. Wang, and F. Blaabjerg, "Transformerless z-source four-leg pv inverter with leakage current reduction," *IEEE Trans. Power Electron.*, vol. 34, no. 5, pp. 4343–4352, May 2019.

[9] K. Li, Y. Shen, Y. Yang, Z. Qin, and F. Blaabjerg, "A transformerless single-phase symmetrical Z-source HERIC inverter with reduced leakage currents for PV systems," in *Proc. APEC*, Mar. 2018, pp. 356–361.

[10] X. Guo, J. Zhou, R. He, X. Jia, and C. A. Rojas, "Leakage current attenuation of a three-phase cascaded inverter for transformerless grid-connected PV systems," *IEEE Trans. Ind. Electron.*, vol. 65, no. 1, pp. 676–686, Jan. 2018.

[11] X. Guo, X. Zhang, H. Guan, T. Kerekes, and F. Blaabjerg, "Three phase ZVR topology and modulation strategy for transformerless PV system," *IEEE Trans. Power Electron.*, pp. 1–1, 2018.

[12] H. Li, Y. Zeng, B. Zhang, Q. Zheng, R. Hao, and Z. Yang, "An improved H5 topology with low common-mode current for transformerless PV grid-connected inverter," *IEEE Trans. Power Electron.*, pp. 1–1, 2018.

[13] R. Rahimi, S. Farhangi, B. Farhangi, G. R. Moradi, E. Afshari, and F. Blaabjerg, "H8 inverter to reduce leakage current in transformerless three-phase grid-connected photovoltaic systems," *IEEE J. Emerg. Sel. Top. Power Electron.*, vol. 6, no. 2, pp. 910–918, Jun. 2018.

[14] L. Wang, Y. Shi, Y. Shi, R. Xie, and H. Li, "Ground leakage current analysis and suppression in a 60-kw 5-level T-Type transformerless SiC PV inverter," *IEEE Trans. Power Electron.*, vol. 33, no. 2, pp. 1271–1283, Feb. 2018.

[15] Y. Zhou and H. Li, "Analysis and suppression of leakage current in cascaded-multilevel-inverter-based PV systems," *IEEE Trans. Power Electron.*, vol. 29, no. 10, pp. 5265–5277, Oct. 2014.

[16] J. C. Giacomini, L. Michels, H. Pinheiro, and C. Rech, "Active damping scheme for leakage current reduction in transformerless three-phase grid-connected PV inverters," *IEEE Trans. Power Electron.*, vol. 33, no. 5, pp. 3988–3999, May 2018.

[17] E. Serban, C. Pondiche, and M. Ordonez, "Modulation effects on power-loss and leakage current in three-phase solar inverters," *IEEE Trans. Energy Convers.*, vol. 34, no. 1, pp. 339–350, Mar. 2019.

[18] C. T. Morris, D. Han, and B. Sarlioglu, "Reduction of common mode voltage and conducted EMI through three-phase inverter topology," *IEEE Trans. Power Electron.*, vol. 32, no. 3, pp. 1720–1724, Mar. 2017.

[19] H. Li, Y. Zeng, B. Zhang, T. Q. Zheng, R. Hao, and Z. Yang, "An improved h5 topology with low common-mode current for transformerless PV grid-connected inverter," *IEEE Trans. Power Electron.*, vol. 34, no. 2, pp. 1254–1265, Feb. 2019.

[20] L. Zhang, K. Sun, Y. Xing, and M. Xing, "H6 transformerless full-bridge PV grid-tied inverters," *IEEE Trans. Power Electron.*, vol. 29, no. 3, pp. 1229–1238, Mar. 2014.

TABLE II
COMPARISON OF SELECTED TOPOLOGIES AND MODULATION METHODS.

Topology	Component counts				Modulation method	Leakage current	CMV	Filter counts		Efficiency
	IGBT/MOSFET	Diode	Capacitor	Inductor				Capacitor	Inductor	
ZSI-D [32]	6	2	2	2	OPWM	3.11 mA	0 or 150 V	0	3	96%
ZSI-S [33]	8	0	2	2	OPWM	2 mA	100 V	0	3	NM
HERIC-ZSI [9]	6	2	2	2	Modified PWM	16.6 mA	NM	0	2	NM
Modified qZSI [34]	6	1	2	2	Modified PWM	NM	89 V	0	2	91%
semi ZSI [35]	2	0	2	1	Modified PWM	NM	NM	0	0	95%
Modified qZSI [30]	6	1	2	3	OPWM	4 mA	170 V	0	3	NM
qZSI [31]	6	1	2	2	CASVM	0.38 A	NM	3	6	NM
Four-leg ZSI [8]	8	2	2	2	3D-SVPWM	28.2 mA	210 V	4	4	NM
qZSI t-type [37]	12	2	4	4	Modified SVM	NM	64.2 V	3	3	90.5%

[21] E. Akpnar, A. Balkc, E. Durbaba, and B. T. Azizolu, “Single-phase transformerless photovoltaic inverter with suppressing resonance in improved H6,” *IEEE Trans. Power Electron.*, vol. 34, no. 9, pp. 8304–8316, Sep. 2019.

[22] L. Concari, D. Barater, G. Buticchi, C. Concari, and M. Liserre, “H8 inverter for common-mode voltage reduction in electric drives,” *IEEE Trans. Ind. Appl.*, vol. 52, no. 5, pp. 4010–4019, Sep. 2016.

[23] X. Wu, G. Tan, Z. Ye, Y. Liu, and S. Xu, “Optimized common-mode voltage reduction PWM for three-phase voltage-source inverters,” *IEEE Trans. Power Electron.*, vol. 31, no. 4, pp. 2959–2969, Apr. 2016.

[24] E. Un and A. M. Hava, “A near-state pwm method with reduced switching losses and reduced common-mode voltage for three-phase voltage source inverters,” *IEEE Trans. Ind. Appl.*, vol. 45, no. 2, pp. 782–793, Mar. 2009.

[25] A. M. Hava and E. n, “A high-performance PWM algorithm for common-mode voltage reduction in three-phase voltage source inverters,” *IEEE Trans. Power Electron.*, vol. 26, no. 7, pp. 1998–2008, Jul. 2011.

[26] H. Chen and H. Zhao, “Review on pulse-width modulation strategies for common-mode voltage reduction in three-phase voltage-source inverters,” *IET Power Electron.*, vol. 9, no. 14, pp. 2611–2620, 2016.

[27] M. Cacciato, A. Consoli, G. Scarcella, and A. Testa, “Reduction of common-mode currents in PWM inverter motor drives,” *IEEE Trans. Ind. Appl.*, vol. 35, no. 2, pp. 469–476, Mar. 1999.

[28] F. Z. Peng, “Z-source inverter,” *IEEE Trans. Ind. Appl.*, vol. 39, no. 2, pp. 504–510, Mar. 2003.

[29] J. Anderson and F. Z. Peng, “Four quasi-Z-source inverters,” in *Proc. IEEE-IAS*, Jun. 2008, pp. 2743–2749.

[30] N. Noroozi and M. R. Zolghadri, “Three-phase quasi-Z-source inverter with constant common-mode voltage for photovoltaic application,” *IEEE Trans. Ind. Electron.*, vol. 65, no. 6, pp. 4790–4798, Jun. 2018.

[31] N. Noroozi, M. Yaghoubi, and M. Zolghadri, “A modulation method for leakage current reduction in a three-phase grid-tie quasi-Z-source inverter,” *IEEE Trans. Power Electron.*, pp. 1–1, 2018.

[32] F. Bradaschia, M. C. Cavalcanti, P. E. P. Ferraz, F. A. S. Neves, E. C. dos Santos, and J. H. G. M. da Silva, “Modulation for three-phase transformerless Z-source inverter to reduce leakage currents in photovoltaic systems,” *IEEE Trans. Ind. Electron.*, vol. 58, no. 12, pp. 5385–5395, Dec. 2011.

[33] P. E. P. Ferraz, F. Bradaschia, M. C. Cavalcanti, F. A. S. Neves, and G. M. S. Azevedo, “A modified Z-source inverter topology for stable operation of transformerless photovoltaic systems with reduced leakage currents,” in *Proc. XI BPEC*, Sep. 2011, pp. 615–622.

[34] M. Meraj, S. Rahman, A. Iqbal, and L. Ben-Brahim, “Common mode voltage reduction in a single-phase quasi Z-source inverter for transformerless grid-connected solar PV applications,” *IEEE J. Emerg. Sel. Top. Power Electron.*, vol. 7, no. 2, pp. 1352–1363, Jun. 2019.

[35] T. Ahmed and S. Mekhilef, “Semi-Z-source inverter topology for grid-connected photovoltaic system,” *IET Power Electron.*, vol. 8, no. 1, pp. 63–75, 2015.

[36] S. Ahmad, T. Ahmed, S. Mekhilef, S. Saha, N. A. Islam, U. Arafat, and H. R. Hashi, “Hardware implementation of grid connected transformerless semi-Z-source inverter topology to mitigate common mode leakage current and THD,” in *Proc. ICAEE*, Dec. 2015, pp. 221–225.

[37] C. Qin, C. Zhang, A. Chen, X. Xing, and G. Zhang, “A space vector modulation scheme of the quasi-Z-source three-level T-type inverter for common-mode voltage reduction,” *IEEE Trans. Ind. Electron.*, vol. 65, no. 10, pp. 8340–8350, Oct. 2018.